FYS4150 Term Project 3: Penning Trap

Stian Aannerud*
(Dated: October 25, 2021)

In this project we successfully created a numerical simulation of a Penning trap for $^{48}Ca^{+}$ atoms. Starting by simulating a single then two particles, we tested the trap. We derived formulas for an analytical solution and used it for error analysis, showing the differences in error for different time steps and methods of integration. Finally we performed an actual experiment involving a periodic electric field, showing how different frequencies affected particle retention in the trap. A resonance around $\omega_V \approx 0.4$MHz was found, but the deep analysis was outside the scope of this project.

I. INTRODUCTION

The goal of this project is implementing a simulation of a Penning trap as an exercise in programming, and performing some rudimentary error analysis and an experiment. A Penning trap is a fantastic contraption which uses electric and magnetic field to trap charged particles by leading them in circular motions. To replicate this as a simulation we will use mathematical models of these fields together with two methods of integration. We will also implement inter-particle Coulomb forces for multi particle simulations. We will derive an analytical solution for the case of a single particle, then use this for analysing the relative error and convergence rate for different numerical time steps. Finally we will wrap it up by actually testing an experiment where we implement a time dependent electric potential.

II. METHODS

Our simulation of the Penning trap is governed by two mayor sets of equations: Equations describing the electric and magnetic fields, and the integration methods used to move the system in time. In section II A we derive the fields and resulting forces, which are later used in the integration covered in section II B. Here two methods of integration are covered: The simple forward Euler method, and the 4th order Runge-Kutta method.

To check our results we also derive an analytical solution and use this to look at the error and convergence rate. Using the equations of motion we find an analytical solution of a single particle (in static, infinite fields), covered in section II C. From this we calculate the relative error and convergence rate, comparing the effect of the time step in numerical integration for our methods. This is covered in section II D.

A. Electric and Magnetic fields

Starting with the electric field, we express this in terms of the electric potential: [1]

$$\vec{E} = -\nabla V \tag{1}$$

$$V(x,y,z) = \frac{V_0}{2d^2}(2z^2 - x^2 - y^2) \tag{2}$$

$$\Rightarrow \vec{E} = -\left[\frac{\partial}{\partial x}, \frac{\partial}{\partial y}, \frac{\partial}{\partial z}\right] V \tag{3}$$

$$\vec{E} = \frac{V_0}{d^2}\,[x, y, -2z] \tag{4}$$

Where the constant d is the *characteristic dimension*, a property describing the size of the system, and V_0 is the potential applied to the Penning trap electrodes. For most of the project this potential is constant, but we later investigate effects of a time dependent field. This time dependent potential replaces the constant as:

$$V_0 \to V_0(1 + f\cos(\omega_V t)) \tag{5}$$

$$\vec{E} = \frac{V_0}{d^2}\,(1 + f\cos(\omega_V t))\,[x, y, -2z] \tag{6}$$

The electric field then evolves with time depending on the amplitude f and angular frequency ω_V. Note that for $f = 0$ we simply get the constant field as before (4).

Since the electric field is not enough to keep the particles contained, we also introduced a magnetic field. This field however is much simpler than the electric field. The magnetic field is a constant size along a single axis, determined by the magnetic field strength B_0: [1]

$$\vec{B} = [0, 0, B_0] = B_0\hat{e}_z \tag{7}$$

These fields come together as the Lorentz force. A charged particle moving through electric and magnetic fields with velocity $\vec{v}$ and charge q, will experience a force given as: [1]

$$\vec{F} = q\left(\vec{E} + \vec{v} \times \vec{B}\right) \tag{8}$$

* Code Repository: https://github.com/Stia4/FYS4150/tree/main/Project%203

As we introduce multiple particles into our system, we also take into account the electrical forces between them. These forces are described by Coulomb's law, which we express in vector form:

$$\vec{F}_1 = k_e q_1 q_2 \frac{\vec{r}_1 - \vec{r}_2}{|\vec{r}_1 - \vec{r}_2|^3} \tag{9}$$

Where $\vec{F}_1$ is the force experienced on particle 1 from particle 2. The constant k_e is the Coulomb constant, while $q, \vec{r}$ are the charge and position of the particles. For a set of many particles, the force experienced on a given particle i from all others is then:

$$\vec{F}_i = k_e q_i \sum_{j \neq i} q_j \frac{\vec{r}_i - \vec{r}_j}{|\vec{r}_i - \vec{r}_j|^3} \tag{10}$$

With the index j denoting the other particles in the system.

All these forces come together with Newtons second law, giving us the total acceleration used in our simulation for a particle i at time t_i:

$$\sum \vec{F} = m\vec{a} \tag{11}$$

$$\vec{a}_i(t_i) = \frac{q_i}{m_i}\left(\vec{E}(\vec{r}_i, t_i) + \vec{v}_i \times \vec{B}(\vec{r}_i)\right) + k_e \frac{q_i}{m_i} \sum_{j \neq i} q_j \frac{\vec{r}_i - \vec{r}_j}{|\vec{r}_i - \vec{r}_j|^3} \tag{12}$$

B. Differential methods

Common for both methods of integration are the equations we solve. We start with the second derivative of position, which is a second degree differential equation relating it to the acceleration. Then we simplify this by introducing the velocity and rewriting the equation to two connected first order differential equations:

$$\frac{\mathrm{d}^2\vec{r}}{\mathrm{d}t^2} = \vec{a}(t) \Rightarrow \begin{cases} \dfrac{\mathrm{d}\vec{r}}{\mathrm{d}t} = \vec{v}(t) \\ \dfrac{\mathrm{d}\vec{v}}{\mathrm{d}t} = \vec{a}(t) \end{cases} \tag{13}$$

Here we have an initial value problem, with initial values for position and velocity set by each particle in the system:

$$\vec{r}(t=0) = \vec{r}_0 \tag{14}$$
$$\vec{v}(t=0) = \vec{v}_0 \tag{15}$$

Starting with the Euler method, also called the forward Euler method, is a simple numerical scheme of integration. The purpose of the Euler method in this project is to have an easy method of integration for implementation testing and comparison with the more complex Runge-Kutta 4th order method. Discretizing our equations and truncating the error, the Euler method becomes: [2, eq. 8.6]

$$\vec{r}_{i+1} = \vec{r}_i + \vec{v}_i \mathrm{d}t \tag{16}$$
$$\vec{v}_{i+1} = \vec{v}_i + \vec{a}_i \mathrm{d}t \tag{17}$$

Where the indexes i and $i+1$ represent the variable at times $t_i = t_0 + i\mathrm{d}t$ and $t_{i+1} = t_i + \mathrm{d}t$ respectively. A scheme of this form has an expected global/total error of order $O(h)$, with h being the step size $\mathrm{d}t$.

The Runge-Kutta 4th order method, also simply called the Runge-Kutta method or "RK4" for short, is a more complex method involving half-step calculations. This is intended to be the more precise method, as it has an expected global error of order $O(h^4)$. The scheme of this method for our coupled system of equations is as follows: [2, eqs. 8.9-8.13]

$$k_{1,r} = \vec{v}_i \mathrm{d}t \tag{18}$$
$$k_{1,v} = \vec{a}(t_i, \vec{r}_i)\mathrm{d}t \tag{19}$$

$$k_{2,r} = (\vec{v}_i + k_{1,v}/2)\mathrm{d}t \tag{20}$$
$$k_{2,v} = \vec{a}(t_i + \mathrm{d}t/2, \vec{r}_i + k_{1,r}/2)\mathrm{d}t \tag{21}$$

$$k_{3,r} = (\vec{v}_i + k_{2,v}/2)\mathrm{d}t \tag{22}$$
$$k_{3,v} = \vec{a}(t_i + \mathrm{d}t/2, \vec{r}_i + k_{2,r}/2)\mathrm{d}t \tag{23}$$

$$k_{4,r} = (\vec{v}_i + k_{3,v})\mathrm{d}t \tag{24}$$
$$k_{4,v} = \vec{a}(t_i + \mathrm{d}t, \vec{r}_i + k_{3,r})\mathrm{d}t \tag{25}$$

$$r_{i+1} = r_i + \frac{1}{6}\left(k_{1,r} + 2k_{2,r} + 2k_{3,r} + k_{4,r}\right) \tag{26}$$
$$v_{i+1} = v_i + \frac{1}{6}\left(k_{1,v} + 2k_{2,v} + 2k_{3,v} + k_{4,v}\right) \tag{27}$$

Where the values k_{1-4} are the mid-steps for velocity and position, used to calculate the next step using a weighted average.

Despite having a drastically larger amount of operations per time step, the number of operations is still linear with step count. This means we should expect the RK4 method to perform more efficiently than the Euler method in terms of precision, as the error decreases expo-

nentially ($O(h^4)$ vs. $O(h)$) while the operations required only increases linearly. We later compare these numerical methods using the relative error and convergence rate described in section II D to see the resulting precision for the case of a single particle (see results section III C).

C. Analytical solution

For a single particle we can derive an analytical expression to describe its movement in the trap. The actual derivation is quite long, and has been moved to Appendix A. Following the methodology described, we come to the final expressions:

$$x(t) = A_+ \cos(-\omega_+ t) + A_- \cos(-\omega_- t) \tag{28}$$
$$y(t) = -A_+ \sin(-\omega_+ t) - A_- \sin(-\omega_- t) \tag{29}$$
$$z(t) = z_0 \cos(\omega_z t) \tag{30}$$
$$A_{+/-} = \frac{v_0 + \omega_{+/-} x_0}{\omega_- - \omega_+} \tag{31}$$
$$\omega_{+/-} = \frac{\omega_0 + / - \sqrt{\omega_0^2 - 2\omega_z^2}}{2} \tag{32}$$

The purpose of this is to have a known solution to which we can compare our numerical simulations. As such it will only be used as part of the methods used in the following section about error analysis II D.

D. Error analysis

To get an estimate of the accuracy of our simulations, we use a couple methods of error analysis. We compare the effects of different integration methods (covered in section II B) and size of time step. For both methods we use the previously derived analytical solution to find the absolute error for the case of a single particle.

The first method we use is the relative error. It is the absolute difference between our numerical simulation and the analytical solution, then divided by the analytical solution:

$$\text{Rel.error} = \frac{|\vec{r}_{\text{exact}} - \vec{r}|}{|\vec{r}|} \tag{33}$$

Where r is the our numerical calculation and r_{exact} is the analytical solution. This gives the error proportional to the actual baseline, meaning a value of 0.1 is equivalent of a 10% error. We will use this to look at the error for different sizes of time step, while also comparing between numerical methods.

Next is the convergence rate, which is a measure of the rate the absolute error converges for decreasing (better) time step. For this we will use five different time steps, meaning the equation is only applicable for this amount of steps: [1]

$$r_{\text{err}} = \frac{1}{4} \sum_{k=2}^{5} \frac{\log(\Delta_{\max,k} / \Delta_{\max,k-1})}{\log(h_k / h_{k-1})} \tag{34}$$
$$\Delta_{\max,k} = \max_i(|\vec{r}_{i,\text{exact}} - \vec{r}_i|) \tag{35}$$

Where $\max_i$ indicates the maximum absolute error across the entire simulation, with index i at time t_i. h_k is time step size number k in list of time step sizes length 5.

E. Further considerations

As we simulate the movement of particles, there are a few checks we perform to control the system. Since a Penning Trap is a finite object, the electric and magnetic fields do not stretch beyond the physical apparatus. For the initial tests of a one or two particles we do not take this into account, but later we wish to look at the effect of a time-dependent electric potential in constraining many particles. Therefore we approximate the bounds of the fields to a sphere of radius d, the characteristic dimension introduced as part of the potential (2). Should the particles go beyond this limit they will be considered "escaped" and will no longer be affected by the fields.

III. RESULTS AND DISCUSSION

As part of the project we performed three main sets of experiments. Firstly we did a set of single particle simulations to check that the motion caused by the fields are as expected, covered in section III A. Then we simulated the movements of a duo of particles to check the effects of the Coulomb forces, see section III B. Returning to a single particle in section III C, we use the analytical solution and methods of error analysis to compare methods of integration and effects of different sizes of time step. Finally we do an actual experiment in section III D where we simulated 100 particles with a time-dependent electric field, and we discuss the effect of field amplitude and frequency on retention of particles.

For all simulations we used a particle with mass $m = 48\text{u}$ and charge $q = 1\text{e}$, approximating a $^{48}\text{Ca}^+$ atom. Parameters used in simulations can be seen in table TABLE I. Initial simulations for one and two particles are calculated with a time step $\text{d}t = 0.001\mu\text{s}$ for a total time of $100\mu\text{s}$, while the final simulations in section III D use a time step $\text{d}t = 0.01\mu\text{s}$ and total time $100\mu\text{s}$.

In addition to the plots used for illustration we also created a couple animations of the single and double particle simulations. As these are not well suited to display on a static document, they can be found as part of the code repository for this project (see footnote in authors).

	SI Value	SI Unit	System Value	System Unit
m	$7.97 \cdot 10^{-26}$	kg	48	u
q	$1.60 \cdot 10^{-19}$	C	1	e
V_0	10	V	$9.65 \cdot 10^{7}$	$\frac{u(\mu m)^2}{(\mu s)^2 e}$
B_0	1	T	$9.65 \cdot 10^{1}$	$\frac{u}{(\mu s)e}$
d	1	cm	10^4	μm
k_e	$8.99 \cdot 10^{9}$	$\frac{Nm^2}{C^2}$	$1.39 \cdot 10^{5}$	$\frac{u(\mu m)^3}{(\mu s)^2 e}$
V_0^*	0.0025	V	$2.41 \cdot 10^{4}$	$\frac{u(\mu m)^2}{(\mu s)^2 e}$
d^*	0.05	cm	500	μm

TABLE I. Parameters used in simulations. Symbols marked $*$ are parameters used in the final simulations in section III D.

They can be especially useful in the case of a two particle system, as interpreting the movement from a line plot can be arduous.

A. Single particle

Our initial simulation was a single particle with initial conditions $x_0 = z_0 = 1\mu$m, $v_0 = 1\mu$m/μs. The movement of this particle can be seen in FIG. 1. We can see that the movement of the particle is as expected, with the Penning trap leading the charged particle in a circular motion with smaller sub-circles due to the interplay of the electric and magnetic field. The motion along the z-axis goes as a cosine function, which was our result in the analytical case for the same initial conditions. The rate at which the particle swings around $z = 0$ corresponds with our value of $\omega_z = qB_0/m \approx 2$MHz, as the curve has a period of $\approx 12.5\mu s \approx 2\pi\omega_z$.

We also visualized this motion in a 3D plot, seen in FIG. 2. Here we can see that the loops seen in the xy plot actually curve along the z-axis as well. An animation of this same simulation is included with the code repository of this project.

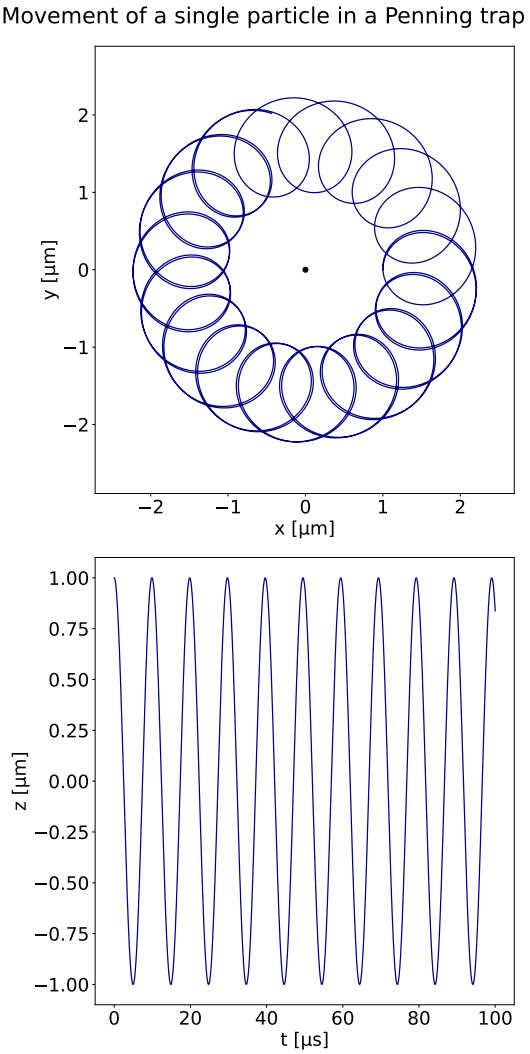

FIG. 1. Motion of a single $^{48}Ca^+$ atom in a simulated Penning trap. TOP: Position in the xy plane. BOTTOM: Position along z axis as function of time.

B. Two particles

The natural continuation of simulating a single particle is naturally simulating two particles! We position the two particles on opposing sides, each with distance 1μm to the centre of the trap. Notably though is their opposite initial position along the z-axis of $z_0 = \pm 1\mu$m, and their lack of initial velocity $v_0 = 0$.

Two simulations are performed. Firstly is the control case where Coulomb forces are disabled, acting as a control check. This can be seen in FIG. 3., where the lack of initial velocity causes a pattern resembling a flower for each particle. There is seemingly no interaction between the particles as was the intention.

Enabling the Coulomb forces we can in FIG. 4. see that the particles move along significantly different paths. The initial impression is that the movement seems a lot more chaotic, and the scale has increased dramatically from $1 - 2\mu$m up to 40μm. However the motion is overall clearly symmetrical, which suggests the simulation is acting as it should. This is especially noted in the plot of $z(t)$, where the two particles are symmetrical for $z = 0$.

Combining the motion into a 3D plot, the system is hard to read. Looking at FIG. 5. the lines are tangled, but there is clearly still a symmetry between the particles as we found before. An easier way to visualize the movement is through an animation, which is available through the code repository. There we get a much clearer view that the particles behave as expected and that the simulation works well.

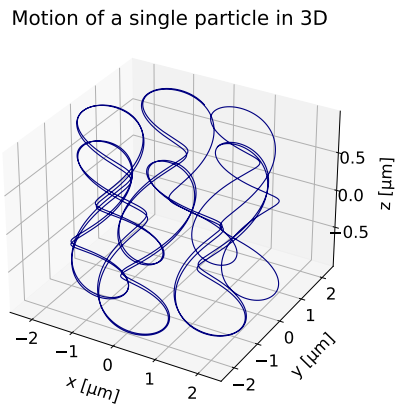

FIG. 2. Motion of a single $^{48}Ca^{+}$ atom in a simulated Penning trap. Plotted as a line plot in 3D.

C. Numerical errors

Returning to the single particle case we perform the same simulation multiple times for different time steps and integration methods. All time steps were of form 10^n, where n is an integer in span $[0, -4]$, resulting in 5 different steps. The integration methods used are the Runge-Kutta 4th order method and forward Euler method described in section II B.

Calculating the relative error in each time step, we plot it for each size of time step as function of time for each integration method. First is the Runge-Kutta 4th order method, plotted for relative error in FIG. 6. Here we see that the relative error decreases approximately linearly with time step, as a tenfold decrease in time step results in a tenfold decrease in error. The error for a given time step also fairly consistent across the time interval, with the exception of at the very end. Time steps $\leq 0.1\mu$s cause a sudden decrease at the very end. There is also a slight negative trend as time passes, which is opposite of what is expected. Comparing with other students who performed the same project, it seems as if the time-axis is reversed for this experiment. This is likely an overlooked error in implementation/plotting, but which has not yet been caught at time of writing.

Continuing to the method of forward Euler in FIG. 7., we see a clear difference in relative error. While the cases of $\mathrm{d}t \leq 0.01\mu$s stay fairly consistent, only increasing a single order of magnitude over the period, two of the cases increase dramatically. The plot had to be constrained to a lower bound as the case for $\mathrm{d}t = 1\mu$s the curve continues with similar trajectory for the entire period. The lower cases perform similarly to the Runge-Kutta method, but there is a significant difference for large time steps indicating better precision using RK4.

Calculating the convergence rate for each method, we get the numbers seen in TABLE II. Here we can see that

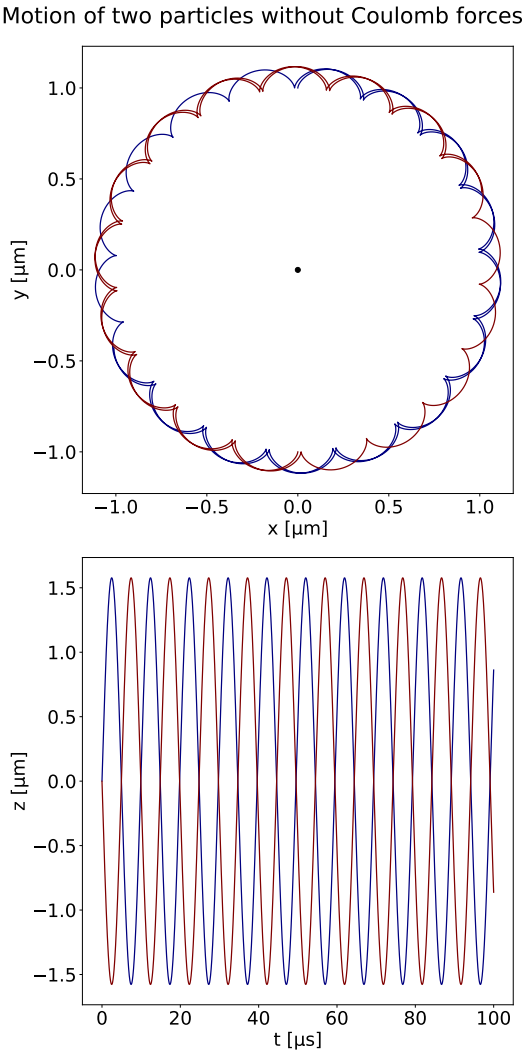

FIG. 3. Movement of two independent particles in a simulated Penning trap. TOP: Position in the xy plane. BOTTOM: Position along z-axis as function of time.

the Runge-Kutta method converges at a rate which reflects what we saw earlier in FIG. 6., as the error decreases nearly linearly with time step. This is not the case for the Euler method however, as it returns a value of 8.75. This means we get an eight-nine fold decrease in error for a similar decrease in time step. Though this is likely not a good representation of the actual rate, as we see in FIG. 6. that the rate changes as $\mathrm{d}t$ decreases. Calculating the convergence again only for the lower four/three time steps (denoted as $1-4$ and $1-3$ in table) we near a value which is more as expected. The final value is lower than the case for RK4, which would indicate a slower convergence, but this is also less credible as the number of steps sampled is much lower.

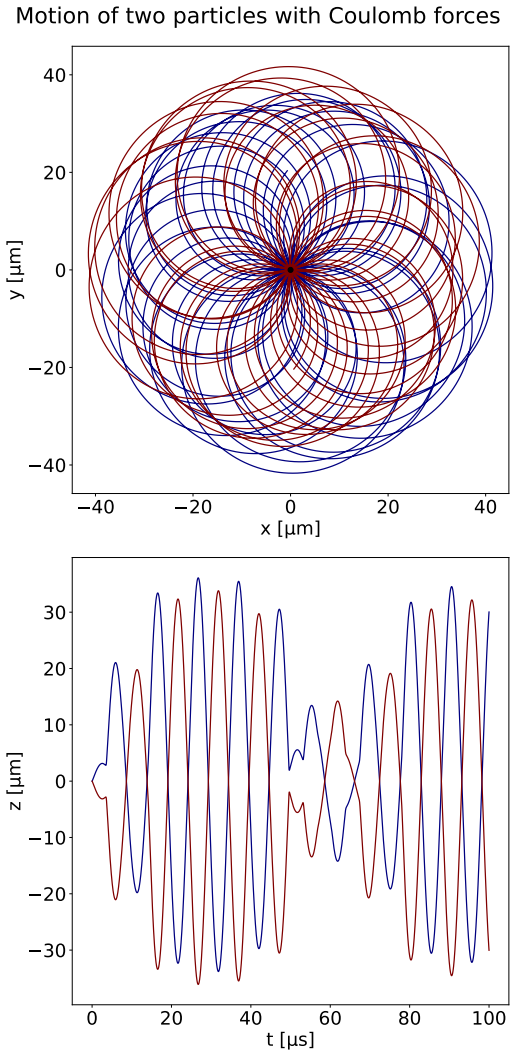

FIG. 4. Movement of two particles connected by Coulomb forces in a simulated Penning trap. TOP: Position in the xy plane. BOTTOM: Position along z-axis as function of time.

RK4	Euler	Euler $1-4$	Euler $1-3$
0.97	8.75	2.37	0.61

TABLE II. Convergence rate for different methods of integration. Numbers show which time steps were used for calculation, starting at lower end.

D. Periodic potential

Finally we get to the main physics experiment of the project. We introduce a time dependent electric potential and use a set of 100 randomly distributed particles. In addition we use the cutoff for forces described in section II E, as the main purpose of this experiment was to investigate the number of remaining particles after the simulation. A set seed was used for all simulations, meaning a random but same starting point was used to eliminate

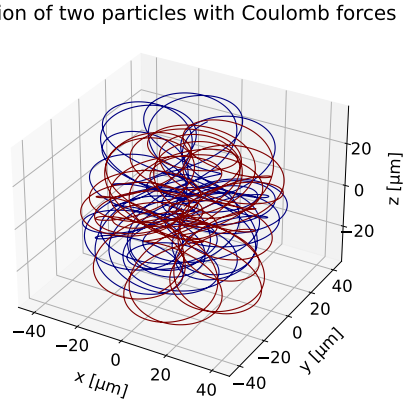

FIG. 5. Movement of two particles connected by Coulomb forces in a simulated Penning trap. Plotted as a line plot in 3D.

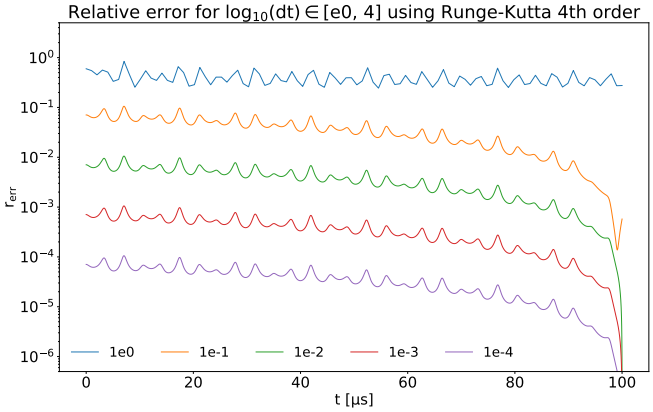

FIG. 6. Plot of relative error as function of time using Runge-Kutta integration method. The different colored lines correspond to different time steps, marked by the legend at the bottom of the figure.

it as a cause. The Coulomb forces were disabled for the initial experiment, but were re-enabled for the second simulation.

We simulated 100 particles for a period of 500μs and counted the number of particles remaining for different fields. The different fields were determined by a set of 230 frequencies $\omega_V \in [0.2, 2.5]$MHz for a step of 0.01MHz. This was done for three different amplitudes $f = 0.1, 0.4, 0.7$. We plotted the number of remaining particles in distance $|\vec{r}| \leq d^*$ as function of ω_V which can be seen in FIG. 8. Here we can clearly see there is a large amount of particles which escape for $\omega_V \approx 0.4$MHz, as well as another dip for $\omega_V \approx 2.0$MHz and $\omega_V \approx 0$MHz. Increasing amplitude f seems to increase amount of particles escaping, indicating that it is the field causing this. Since these dips appear at multiples of 0.4MHz, there is

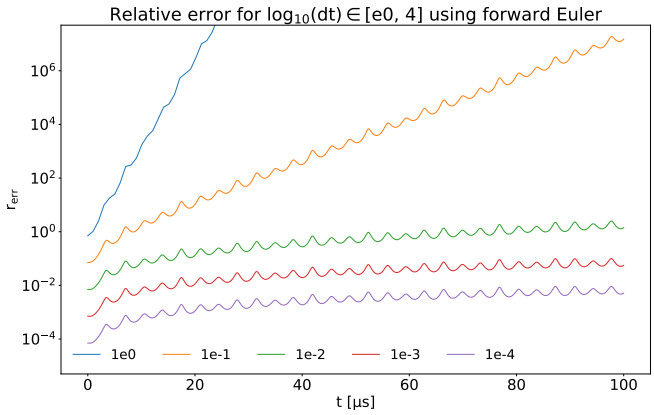

FIG. 7. Plot of relative error as function of time using forward Euler integration method. The different colored lines correspond to different time steps, marked by the legend at the bottom of the figure.

reason to indicate the particles escaping is related to the resonance of the field. Though this is outside the scope of this project.

Zooming in on the largest dip in interval $\omega_V \in [0.3, 0.5]$ we performed another simulation of the same type with result seen in FIG. 9. The relative resolution was increased, as 100 steps was used resulting in a step size of 0.002MHz. We also did two simulations: With and without Coulomb forces enabled. Here we can see that the effects of this is an overall decreased amount of particles remaining, as well as structural changes. The overall shape is similar to the case without forces, but the left side has notably changed from a sudden drop to a slope.

IV. CONCLUSION

Overall the project was a major success. The goal of developing a model of a Penning trap and simulating the movement of particles was accomplished. We managed to simulate paths which made sense with the expected movement of one and two particles, and we used this to look at the effects of integration method and time step. Our final physics experiment had interesting results, and while the fine analysis was outside the scope of this project it leaves room for interpretation in the future.

Future improvements of this project could implement more physical effects and new methods of integration and analysis. Adding relativistic effects such as time retardation would be possible, but a closer look at the particle speeds should be done to see if this is reasonable. Similarly the magnetic field from ions in motion could be implemented as another effect between particles. Finally other methods of integration could be implemented both for comparison and increased performance.

. . .

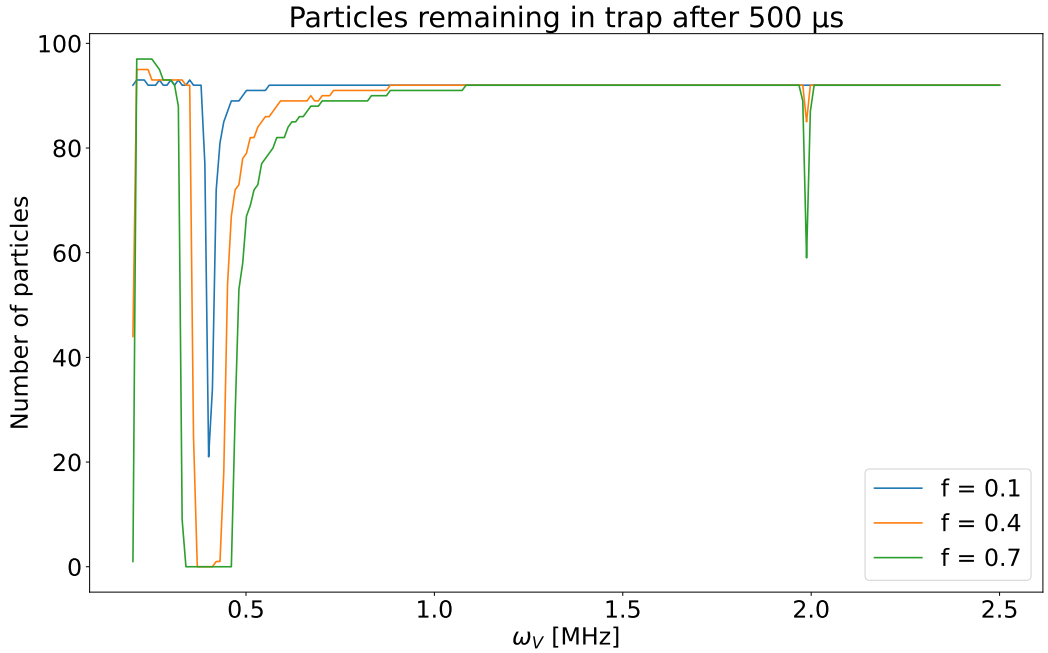

FIG. 8. Plot number of particles remaining in a simulated Penning Trap after 500μs as function of frequency ω_V. Different colored lines indicate different amplitudes f.

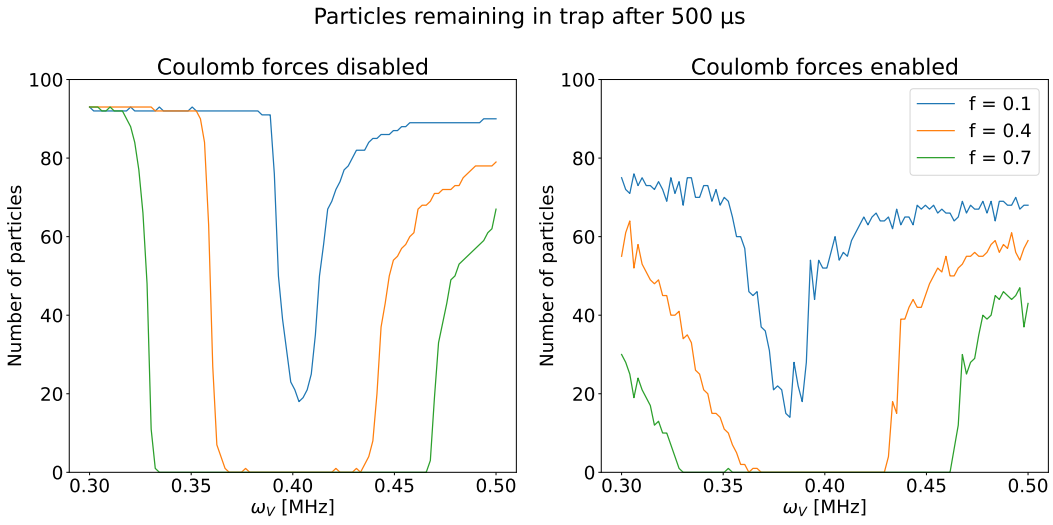

FIG. 9. Plot number of particles remaining in a simulated Penning Trap after 500μs as function of frequency ω_V. Different colored lines indicate different amplitudes f. Continuation with closeup of interval $\omega_V \in [0.3, 0.5]$MHz. LEFT: Coulomb forces disabled. RIGHT: Coulomb forces disabled.

[1] The FYS3150 teaching team. Project 3. https://anderkve.github.io/FYS3150/book/projects/project3.html, 2021. [Online; accessed 23-October-2021].

[2] M. Hjorth-Jensen. *Computational Physics*. Lecture notes, 2015.

Appendix A: Deriving analytical solution

Using Newton's second law we express the acceleration from the Lorentz force (8):

$$\vec{a}(t) = \frac{q}{m}\left(\vec{E}(\vec{r},t) + \vec{v}\times\vec{B}(\vec{r})\right) \tag{A1}$$

We note that this is the same expression found earlier for a system of particles (12), but without the Coulomb forces from other particles. Expanding the expression for the fields and splitting into components gives:

$$\vec{a} = \frac{q}{m}\left(\frac{V_0}{d^2}\left[x,y,-2z\right] + \left[B_0 v_y, -B_0 v_x, 0\right]\right) \tag{A2}$$

$$\ddot{x} = \frac{qV_0}{md^2}x + \frac{qB_0}{m}\dot{y} \tag{A3}$$

$$\ddot{y} = \frac{qV_0}{md^2}y - \frac{qB_0}{m}\dot{x} \tag{A4}$$

$$\ddot{z} = -2\frac{qV_0}{md^2}z \tag{A5}$$

Where the variables with n dots correspond to their n-th time derivatives, e.g. $\frac{\mathrm{d}^2 y}{\mathrm{d}t^2} = \ddot{y}$. We simplify this by defining new coefficients $\omega_0 \equiv \frac{qB_0}{m}, \omega_z^2 \equiv \frac{2qV_0}{md^2}$ and reorganizing terms:

$$\ddot{x} - \omega_0\dot{y} - \frac{1}{2}\omega_z^2 x = 0 \tag{A6}$$

$$\ddot{y} + \omega_0\dot{x} - \frac{1}{2}\omega_z^2 y = 0 \tag{A7}$$

$$\ddot{z} + \omega_z^2 z = 0 \tag{A8}$$

These are the equations of motion to which we find the solution of. We do not use these as part of the numerical simulations, as we simply use the acceleration directly, but we will use the quantities ω_0 and ω_z in analysis and discussion of results. We can see that the z-component has a trivial general solution of form:

$$z = C_1\sin(\omega_z t) + C_2\cos(\omega_z t) \tag{A9}$$

Where C_1, C_2 are constants. However the x and y components require more attention as they are linked by their derivatives $\dot{x}, \dot{y}$. To solve them we introduce a new complex valued function $f(t)$, defined as:

$$f(t) = x(t) + iy(y) \tag{A10}$$

Then we redefine the equations of motion in terms of this function to combine the linked equations into a single expression:

$$y = \frac{1}{i}f - \frac{1}{i}x = -if + ix \tag{A11}$$

$$\dot{y} = i(\dot{x} - \dot{f}) \tag{A12}$$

$$\ddot{y} = i(\ddot{x} - \ddot{f}) \tag{A13}$$

$$\tag{A14}$$

Inserting into equations of motion (A6) and (A7):

$$\ddot{x} - \omega_0 i(\dot{x} - \dot{f}) - \frac{1}{2}\omega_z^2 x = 0 \tag{A15}$$

$$i(\ddot{x} - \ddot{f}) + \omega_0\dot{x} - \frac{1}{2}\omega_z^2 i(x - f) = 0 \tag{A16}$$

We use that an equation equals to zero can be multiplied by any constant and still apply in order to multiply (A16) by $-i$. Then setting both equations equal to each other and canceling terms gives:

$$-i\left[i(\ddot{x}-\ddot{f})+\omega_0\dot{x}-\frac{1}{2}\omega_z^2 i(x-f)\right]=0 \tag{A17}$$

$$=\ddot{x}-\omega_0 i(\dot{x}-\dot{f})-\frac{1}{2}\omega_z^2 x \tag{A18}$$

$$\Rightarrow -\ddot{f}+\frac{1}{2}\omega_z^2 f=\omega_0 i\dot{f} \tag{A19}$$

$$\ddot{f}+i\omega_0\dot{f}-\frac{1}{2}\omega_z^2 f=0 \tag{A20}$$

This is an equation we can solve, with a general solution given as:

$$f(t)=A_+e^{-i\omega_+ t}+A_-e^{-i\omega_- t} \tag{A21}$$

$$\omega_{+-}=\frac{\omega_o\pm\sqrt{\omega_0^2-2\omega_z^2}}{2} \tag{A22}$$

Where the values A_+, A_- are constants. From our definition of the function f from (A10) gives the planar movement $x(t)=\mathrm{Re}f(t), y(t)=\mathrm{Im}f(t)$. However to make sure the movement is bounded in the plane (i.e. $f(t)<\infty$ as $t\to\infty$), we have a few requirements. The function does not trend towards infinity if the exponentials $|e^{-i\omega_\pm t}|$ do not trend towards infinity. This happens as $\omega_+,\omega_-\geq 0$, or:

$$\omega_+,\omega_-\geq 0 \tag{A23}$$

$$\Rightarrow \omega_0\pm\sqrt{\omega_0^2-2\omega_z^2}\geq 0 \tag{A24}$$

$$\Rightarrow \omega_0\geq\sqrt{2}\omega_z \tag{A25}$$

By using the definitions of ω_0,ω_z we cam relate the parameters of the trap to the parameters of the particles:

$$\frac{qB_0}{m}\geq\sqrt{2}\left[\frac{2qV_0}{m_d^2}\right]^{\frac{1}{2}} \tag{A26}$$

$$\Rightarrow \frac{d^2B_0^2}{V_0}\geq 4\frac{q}{m} \tag{A27}$$

Using the definitions of x, y from f, we can calculate the upper and lower bounds of the particle orbital radius in the xy plane:

$$x(t)=\mathrm{Re}f(t) \tag{A28}$$

$$x(t)=A_+\cos(-\omega_+ t)+A_-\cos(-\omega_- t) \tag{A29}$$

$$y(t)=\mathrm{Im}f(t) \tag{A30}$$

$$y(t)=-A_+\sin(-\omega_+ t)-A_-\sin(-\omega_- t) \tag{A31}$$

$$R=\sqrt{x^2+y^2} \tag{A32}$$

$$=\sqrt{A_+^2+2A_+A_-\cos(t(\omega_+-\omega_-))+A_-^2} \tag{A33}$$

Since the terms A_-^2 and A_+^2 are positive constants, the determining factor is the cosine term, which is smallest for $t=0$ and largest for $t(\omega_+-\omega_-)=\pi$, or $t=\pi/(\omega_+-\omega_-)$:

$$R(t=0)=\sqrt{A_+^2+2A_+A_-+A_-^2} \tag{A34}$$

$$=A_++A_- \tag{A35}$$

$$R(t=\pi/(\omega_+-\omega_-))=\sqrt{A_+^2-2A_+A_-+A_-^2} \tag{A36}$$

$$=|A_+-A_-| \tag{A37}$$

Next we define a set of initial conditions to be used for $\vec{r}, \vec{v}$ in order to find the constants used in $x(t), y(t), z(t)$:

$$x(0) = x_0 \qquad \dot{x}(0) = 0 \tag{A38}$$
$$y(0) = 0 \qquad \dot{y}(0) = v_0 \tag{A39}$$
$$z(0) = z_0 \qquad \dot{z}(0) = 0 \tag{A40}$$

We insert these values into the general expression for z (A9):

$$z(0) = z_0 = 0 + C_2 \tag{A41}$$
$$\dot{z}(0) = 0 = C_1\omega_z \cos(\omega_z \cdot 0) - C_2\omega_z \sin(\omega_z \cdot 0) \tag{A42}$$
$$= C_1\omega_z - 0 \tag{A43}$$
$$\Rightarrow z(t) = z_0 \cos(\omega_z t) \tag{A44}$$

Then we find the values of A_+, A_- by doing the same for x, y:

$$x(0) = x_0 = A_+ + A_- \tag{A45}$$
$$\Rightarrow A_+ = x_0 - A_- \tag{A46}$$
$$\dot{y}(0) = v_0 \tag{A47}$$
$$= -A_+\omega_+ \cos(\omega_+ \cdot 0) - A_-\omega_- \cos(\omega_- \cdot 0) \tag{A48}$$
$$v_0 = -A_+\omega_+ - A_-\omega_- \tag{A49}$$
$$v_0 = -(x_0 - A_-)\omega_+ - A_-\omega_- \tag{A50}$$
$$v_0 = -x_0\omega_+ + A_-(\omega_+ - \omega_-) \tag{A51}$$
$$\Rightarrow A_- = \frac{v_0 + x_0\omega_+}{\omega_+ - \omega_-} \tag{A52}$$
$$A_- = -\frac{v_0 + \omega_+ x_0}{\omega_- - \omega_+} \tag{A53}$$
$$A_+ = x0 - A_- = x_0 + \frac{v_0 + \omega_+ x_0}{\omega_- - \omega_+} \tag{A54}$$
$$A_+ = \frac{v_0 + \omega_- x_0}{\omega_- - \omega_+} \tag{A55}$$

Which when inserted into (A29) and (A31) lets us express the movement of a single particle in 3D in a penning trap.